Landau–Zener–Stückelberg interferometry in $\mathcal{PT}$-symmetric optical waveguides

2012 J. Phys. A: Math. Theor. 45 444027

(http://iopscience.iop.org/1751-8121/45/44/444027)

J. Phys. A: Math. Theor. **45** (2012) 444027 (11pp) doi:10.1088/1751-8113/45/44/444027

Landau–Zener–Stückelberg interferometry in $\mathcal{PT}$-symmetric optical waveguides

S A Reyes, F A Olivares and L Morales-Molina

Departamento de Física, Facultad de Física, Pontificia Universidad Católica de Chile, Casilla 306, Santiago 22, Chile

E-mail: sreyes@fis.puc.cl

Received 16 April 2012, in final form 26 June 2012
Published 23 October 2012
Online at stacks.iop.org/JPhysA/45/444027

Abstract

We investigate theoretically the non-adiabatic transitions in a $\mathcal{PT}$-symmetric lattice subject to a strong ac force. In an optical realization of the lattice, the curvature of the waveguides along the paraxial propagation direction plays the role of the external periodic force necessary to drive the system through an avoided level crossing. Analytical expressions for the transition probabilities after multiple passages are obtained within an effective two-mode approximation. We show that gain and losses of the light beam, as well as the relative occupation probabilities of the bands involved in the transitions, can be accurately managed upon tuning the parameters of the system and are particularly sensitive to the amplitude of the non-Hermitian component of the lattice. Numerical simulations for the complete system are found to agree very well with the approximate analytical results.

This article is part of a special issue of *Journal of Physics A: Mathematical and Theoretical* devoted to 'Quantum physics with non-Hermitian operators'.

PACS numbers: 42.25.Hz, 11.30.Er, 05.60.Gg, 73.40.Gk

(Some figures may appear in colour only in the online journal)

1. Introduction

A strongly driven two-level system undergoes a non-adiabatic transition commonly known as Landau–Zener (LZ) tunneling. If the system is driven periodically through its level crossing, the phase accumulated between consecutive LZ transitions may lead to constructive or destructive interference often referred to as Landau–Zener–Stückelberg (LZS) interferometry [1]. Recent observations of LZS interference include ultracold molecular gases [2], optical lattices [3] and nitrogen-vacancy centers [4].

Since an important requirement in quantum mechanics is to have Hermitian Hamiltonian operators, it is in this setting in which LZS interferometry has been studied so far. Such

restriction is *sufficient* to guarantee that the system not only has a real spectrum, but also a unitary evolution conserving probability. Nevertheless, in recent years it has been demonstrated that the Hermiticity requirement $H = H^{\dagger}$ is *not necessary* and that it may be replaced by the physically transparent condition of parity and time reversal ($\mathcal{PT}$) symmetry [5–7]. Thus, it becomes possible in principle to describe processes that do not violate the physical axioms of quantum mechanics by using non-Hermitian $\mathcal{PT}$-symmetric Hamiltonians. A proper definition of an inner product, unitarity, the definition of observables and other important issues related to $\mathcal{PT}$-symmetric systems have been intensively studied [5, 8–12].

On the other hand, new developments in engineered optical waveguides have provided a fertile ground for the experimental realization of classical analogies for a variety of quantum coherent phenomena [13]. The analogy lies in the formal equivalence between the temporal Schrödinger equation for a quantum particle and the wave equation for the spatial propagation of monochromatic light in the scalar and paraxial propagation. A clear technical advantage over quantum systems is that in the optical setting, the wavefunction evolution can be directly observed by simple fluorescence imaging or scanning tunneling optical microscopy. Furthermore, since driven potentials can be achieved by introducing curvature along the propagation direction, optical analogues of quantum phenomena such as coherent destruction of tunneling [14] and Bloch oscillations [15, 16] have been realized experimentally. In this context, it is also possible to realize the complex optical potentials by introducing loss and gain distributions. Particularly interesting is the possibility of realizing and experimentally investigating the aforementioned $\mathcal{PT}$-symmetric systems by using the right combination of gain and loss regions. Recent experiments have realized a $\mathcal{PT}$-symmetric optical system consisting of two coupled parallel $LiNbO_3$ optical waveguides [17]. Providing amplification to only one channel by partially blocking the pump light it is possible to achieve the desired asymmetric gain. These promising results have paved the way for the future synthesis of periodic optical systems that could display unusual properties due to the $\mathcal{PT}$-symmetry.

In this paper, we consider the scenario in which a sinusoidal curvature of the waveguide mimics an ac force applied to a periodic $\mathcal{PT}$-symmetric complex lattice. Recently, driven periodic complex potentials have proven to be a fertile ground for the study of novel phenomena in wave mechanics such as non-conventional Bloch oscillations [18] and dynamic localization [19]. As in Hermitian quantum mechanics, the application of an external force may lead to interband transitions and interference phenomena. However, the time evolution in a complex lattice may be non-unitary, making such transitions fundamentally different. Motivated by these facts, in this work, we provide a detailed study of the non-Hermitian LZS interferometry for a light beam propagating in a $\mathcal{PT}$-symmetric complex crystal. We investigate the problem theoretically using first analytical calculations describing the transitions near the level crossings within a two-mode approximation and then complement those results with numerical simulations. It is shown that the former not only provide insight into the underlying physics, but also compare well with the numerical results. The results obtained reveal that the non-Hermitian part of the Hamiltonian can be used as a novel control parameter to manipulate the intensity of the light beam along the curved waveguides. In an experiment such as the one described in [17], where an optical two-wave mixing gain is used, the amplitude of the imaginary part of the potential can be tuned either by adjusting the intensity of the pump beam or by modifying the concentration of Fe^{3+} on the waveguides.

The paper is organized as follows. First, in section 2 we describe the model for light propagation in a $\mathcal{PT}$-symmetric lattice within the paraxial regime including the curvature which provides the necessary driving field. In section 3, we derive an effective two-level system from which we obtain analytical expressions for the transition probabilities. Later, in section 4 the results for the two-level system are compared to numerical simulations

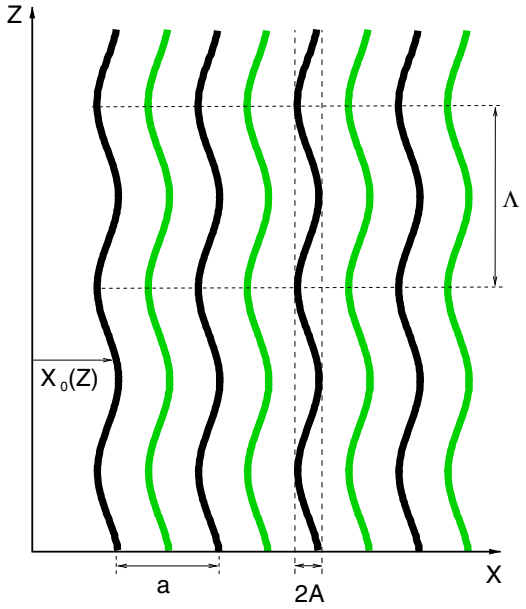

Figure 1. Schematic depiction of the refractive index of the waveguides, composed by real and imaginary parts that vary sinusoidally along the transverse direction (X). The maxima of the real part are marked in black, whereas the maxima of the imaginary part are marked in gray (green). After a coordinate and gauge transformation, the periodic curvature in the propagation direction Z given by $X_0(Z)$ results in the alternate driving force $F(Z)$ (see equation (4)).

for the complete $\mathcal{PT}$-symmetric lattice. Finally, some concluding remarks are included in section 5.

2. The model

Let us consider monochromatic light of vacuum wavelength λ propagating along a guiding structure having a periodic refractive index along its transverse direction, i.e. $n(X) = n(X+a)$. Additionally, the waveguide is sinusoidally curved along the paraxial propagation direction Z such that $n(X, Z) = n(X - X_0(Z))$, where

$$X_0(Z) = A\sin(2\pi Z/\Lambda), \tag{1}$$

(see figure 1). Within the paraxial approximation and after a suitable reference frame and gauge transformation, the equation for the (transformed) electric field amplitude becomes [13]

$$\mathrm{i}\lambda\!\!\!^{-}\partial_Z\psi = -\frac{\lambda\!\!\!^{-2}}{2n_s}\frac{\partial^2\psi}{\partial x^2} + U(x)\psi - F(Z)x\psi \equiv \mathcal{H}_0\psi - F(Z)x\psi, \tag{2}$$

where $\lambda\!\!\!^{-} = \lambda/2\pi$ and $x = X - X_0(Z)$ is the transformed transverse axis. The first part of the potential is given by

$$U(x) \approx n_s - n(x), \tag{3}$$

where n_s is the refractive index of the substrate and $n(x) = n(x+a)$ is the periodic part of the refractive index profile with periodicity a. After the transformations, the axis bending along the paraxial direction results in an alternate driving force

$$F(Z) = n_s A\omega^2\cos(\omega Z), \tag{4}$$

where $\omega = 2\pi/\Lambda$.

For a complex potential, the imaginary part of $U(x)$ renders $\mathcal{H}$ into a non-Hermitian Hamiltonian. In the following, we shall consider $U(x) = U_1 \cos(2\pi x/a) + \mathrm{i}U_2 \sin(2\pi x/a)$, which satisfies $U(x) = U(-x)^*$ and thus $\mathcal{H}_0$ is $\mathcal{PT}$-symmetric [18]. For $U_2 < U_2^{\mathrm{crit}} = U_1$, the spectrum of $\mathcal{H}_0$ has real values; otherwise the bands merge giving place to the pairs of complex conjugate values [20]. Henceforth, we consider $U_2 < U_2^{\mathrm{crit}}$, unless otherwise specified. The eigenfunctions of $\mathcal{H}_0$ are the Floquet–Bloch band mode functions $\phi_{qn}(x)$ with Bloch-momentum q, which fulfil the secular equation $\mathcal{H}_0\phi_{qn}(x) = E_n(q)\phi_{qn}(x)$, where $E_n(q)$ are the eigenenergies corresponding to the nth Floquet–Bloch band. While as in real crystals $E_n(-q) = E_n(q)$, the wavefunctions under the parity transformation $x \to -x$ and $q \to -q$ obey the general relation $\phi^\dagger_{qn}(x) = \phi_{-qn}(-x)$, where $\phi^\dagger_{qn}$ are eigenfunctions of $\mathcal{H}_0^\dagger$. Moreover, as was shown in [20], the orthogonality condition becomes

$$\int_{-\infty}^{\infty} \phi^\dagger_{qn}(x)\phi_{q'm}(x)\,\mathrm{d}x = \mathrm{d}_{qn}\delta(q-q')\delta_{nm}, \tag{5}$$

with $d_{qn} = \pm 1$.

Let us consider as input excitation a plane wave with normal incidence. Hence, the wavefunction can be written as a superposition of the Floquet–Bloch eigenfunctions having the same crystal momentum q, i.e. $\psi_q(x, Z) = \sum_n c_{qn}(Z)\phi_{qn}(x)$, where $\phi_{qn}(x) = w_{qn}(x)\mathrm{e}^{\mathrm{i}qx}$ and $w_{qn}(x + a) = w_{qn}(x)$. Expanding $w_{qn}(x)$ in a Fourier basis, we can write

$$\psi_q(x, Z) = \sum_l a^l_q(Z)\,\mathrm{e}^{\mathrm{i}(2kl+q)x}, \qquad \text{with } k = \pi/a \text{ and } a^l_q(Z) = \sum_n c_{qn}b^l_{qn}.$$

Here, b^l_{qn} with $l = 0, \pm 1, \pm 2, \ldots$ are the coefficients of the Fourier expansion for $w_{qn}(x)$. Substituting this into equations (2) and (3) we obtain the dimensionless equation for the dynamics of a^l_q,

$$\mathrm{i}\frac{\partial a^l_q}{\partial z} = (2l + \tilde{q})^2 a^l_q + (V_1 + V_2)a^{l+1}_q + (V_1 - V_2)a^{l-1}_q, \tag{7}$$

where $z = Z\mathcal{E}_k/\hbar$, $\tilde{q} = q/k$ and $V_j = U_j/2\mathcal{E}_k$, $j = 1, 2$ with $\mathcal{E}_k = \hbar^2k^2/2n_s$. It is convenient to write the evolution equation in the usual quantum mechanics notation

$$\mathrm{i}\partial_z|a_q(z)\rangle = \mathbf{H}|a_q(z)\rangle, \tag{8}$$

where $|a_q(z)\rangle$ is the vector with components a^l_q and

$$\mathbf{H} = \{H_{m,l} = (2l + \tilde{q})^2\delta_{m,l} + (V_1 + V_2)\delta_{m,l-1} + (V_1 - V_2)\delta_{m,l+1}\}. \tag{9}$$

This Hamiltonian matrix is real but non-symmetric and has a real spectrum for values $V_1 > V_2$. From this expression, it is also clear that changing the sign of the amplitude of the imaginary part of the potential V_2 is equivalent to a transposition of $\mathbf{H}$. Note that the problem becomes analogous to the dynamics of a particle moving on a discrete chain with non-symmetric hopping amplitudes ($V_1 + V_2$ and $V_1 - V_2$) and on-site energies given by $(2l + \tilde{q})^2$. Clearly, for positive values of V_2, the system tends to evolve toward modes with higher energies and vice versa. This is a manifestation of the fact that there is an energy gain (loss) for the positive (negative) values of U_2 in the optical system (2). A numerical diagonalization of (9) results in energy bands like the ones shown in figure 2. The diagram of energy versus Bloch-momentum reveals that increasing V_2 causes an approaching of the bands at the avoided crossings, leading to degeneracies at $V_2 = V_1$. In this paper, we study the case where the paraxial axis bending results in the alternate driving force (4), under which the crystal momentum evolves in time as

$$q(Z) = q_0 + n_s A\omega \sin(\omega Z). \tag{10}$$

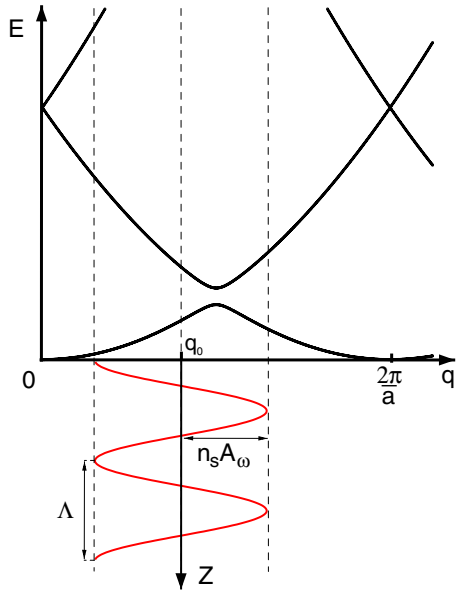

Figure 2. Energy bands of the system as a function of Bloch-momentum q. The vertical axis below the spectrum represents the timelike paraxial propagation direction Z. Curvature along this direction drives the quasimomentum q several times through the level crossing, according to equation (10).

Furthermore, we will focus on the dynamics around a single (avoided) level crossing between the ground and first excited states (see figure 2). Thus, the conditions are such that the time evolution is dominated by an effective two-mode system that we will study further in section 3.

It is important to note that for the $\mathcal{PT}$-symmetric Hamiltonian $\mathcal{H}_0$ the power of the propagating light beam remains constant provided $U_2 < U_2^{\text{crit}}$. If in addition we consider the presence of an external force as in equation (2), then the $\mathcal{PT}$-symmetry is broken and the power is no longer a conserved quantity. Thus, under the action of the force, transitions to other bands may occur that do not conserve the power. Recently, the Gaussian wavepacket dynamics of this system has been analyzed in the presence of a small external force [18]. Also, the dynamics of a single mode under a constant force $F(Z) = F$ of arbitrary strength was investigated in [21].

3. LZS interferometry for a non-symmetric two-mode system

To obtain approximate analytical results for the dynamics, we focus our analysis near the avoided level crossings that appear at the Bragg scattering points $\tilde{q} = (2j + 1)$ with $j = 0, \pm 1, \pm 2, \ldots$. For a small energy separation between the modes involved in a given avoided crossing, one can safely neglect the effects due to any other bands. A suitable description can then be provided in terms of an effective two-mode Hamiltonian. In particular, from matrix (9) and considering the two lowest bands it is possible to obtain the corresponding effective Hamiltonian

$$H = \frac{1}{2}\begin{pmatrix} \epsilon & \Delta + \delta \\ \Delta - \delta & -\epsilon \end{pmatrix}, \tag{11}$$

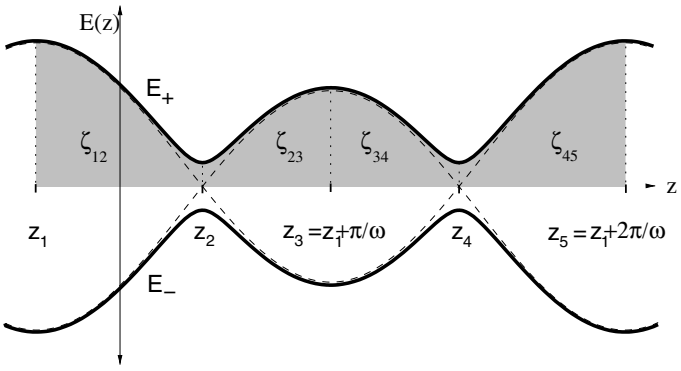

Figure 3. Energy spectrum of the periodically driven two-level system as a function of time. The areas labeled by ζ_{ij} correspond to the dynamical phases the system acquires during the adiabatic part of its evolution between z_i and z_j.

where $\epsilon = 4(1 - 2l - \tilde{q})$, $\Delta = 2V_1$ and $\delta = 2V_2$.[1] Unlike the Hermitian case, in equation (11) $H_{1,2} \neq H^*_{2,1}$ and the eigenvalues can therefore have complex values. By solving the secular equation for (11), we obtain

$$E_\pm = \pm\tfrac{1}{2}\sqrt{\epsilon^2 + (\Delta^2 - \delta^2)}, \tag{12}$$

so that for high values of ϵ the spectrum is real. At $\epsilon = 0$, the gap between the energy levels becomes $E_+ - E_- = \sqrt{\Delta^2 - \delta^2}$. On the other hand, when $\delta^2 > \Delta^2$, purely imaginary eigenvalues arise in the region $\epsilon^2 < (\delta^2 - \Delta^2)$, indicating that the system is beyond the critical point where the $\mathcal{PT}$-symmetry is broken.

As we mentioned above, the presence of a sinusoidal axis bending along the paraxial direction in equation (2) mimics an ac force causing a periodic variation of the Bloch-momentum along the propagation direction as given by equation (10). As a result, the diagonal elements of matrix (11) can be written as

$$\epsilon = \epsilon_0 - \tilde{A}\sin(\tilde{\omega}z), \tag{13}$$

where $\epsilon_0 = 4(1 - 2l - q_0/k)$, $\tilde{\omega} = \omega\tilde{\chi}/\mathcal{E}_k$ and $\tilde{A} = 4n_s A\omega/k = 2A\tilde{\omega}\tilde{\chi}k$. The resulting spectrum is shown in figure 3. To study this periodically driven two-level system, we will use the adiabatic-impulse model, which is convenient when the system is repeatedly driven through one of the avoided crossings located at

$$\tilde{q} = 1 - 2l, \tag{14}$$

where l is an integer. Basically, the idea of this approximation is to consider the evolution as adiabatic away from the avoided crossing and introduce the transition matrix N which captures the non-adiabatic part of the transition. For a detailed treatment of the symmetric (i.e. Hermitian) case, see for instance [22].

We have generalized the conventional calculation for the Hermitian two-level system to the asymmetric case, which naturally arises in the $\mathcal{PT}$-symmetric optical waveguides as shown above. The transition matrix becomes

$$N = \begin{pmatrix} \sqrt{\frac{\Delta+\delta}{\Delta-\delta}}\sqrt{1 - P_{\mathrm{LZ}}}\,\mathrm{e}^{-\mathrm{i}\varphi_S} & \sqrt{P_{\mathrm{LZ}}} \\ -\sqrt{P_{\mathrm{LZ}}} & \sqrt{\frac{\Delta-\delta}{\Delta+\delta}}\sqrt{1 - P_{\mathrm{LZ}}}\,\mathrm{e}^{\mathrm{i}\varphi_S} \end{pmatrix}, \tag{15}$$

[1] In what follows we consider $\Delta > 0$.

where

$$\varphi_S = \frac{\pi}{4} + \gamma(\ln\gamma - 1) + \arg\Gamma(1 - \mathrm{i}\gamma), \tag{16}$$

$$P_{\mathrm{LZ}} = \mathrm{e}^{-2\pi\gamma}. \tag{17}$$

The adiabatic parameter $\gamma = (\Delta^2 - \delta^2)/4v$ indicates how slow the transition is. Considering the periodic driving (13), in the present case the velocity at the avoided crossing is given by

$$v = \tilde{A}\tilde{\omega}\sqrt{1 - \left(\frac{\epsilon_0}{\tilde{A}}\right)}. \tag{18}$$

Let us suppose now that the system is initially prepared in its ground state and then driven several times across the avoided crossing (see figure 2). Using the transition matrix (15), together with the dynamical phases the system picks up during the adiabatic part of the evolution, it is possible to obtain a formula for the probability of encountering the system in the excited state after a number of crossings. For an even number of crossings we obtain

$$P_+^{\mathrm{even}}(n) = 4\left(\frac{\Delta - \delta}{\Delta + \delta}\right)P_{\mathrm{LZ}}(1 - P_{\mathrm{LZ}})\sin^2(\Phi_{St})\frac{\sin^2(n\phi)}{\sin^2(\phi)}, \tag{19}$$

where $2n$ is the number of crossings,

$$\Phi_{St} = \varphi_S + \zeta_{24}, \tag{20}$$

is the so-called Stückelberg phase and ζ_{ij} is the dynamical phase accumulated during the evolution between z_i and z_j (see figure 3). The phase ϕ in (19) is defined by

$$\cos\phi = (1 - P_{\mathrm{LZ}})\cos(\zeta_{15} + 2\varphi_S) + P_{\mathrm{LZ}}\cos(\zeta_{12} + \zeta_{45} - \zeta_{24}). \tag{21}$$

On the other hand, for an odd number of crossings the probability of finding the system in the excited state is

$$P_+^{\mathrm{odd}}(n) = 2Q_1\frac{\sin^2(n\phi)}{\sin^2(\phi)} - Q_2\frac{\sin(2n\phi)}{\sin(\phi)} + P_{\mathrm{LZ}}\cos(2n\phi), \tag{22}$$

where $2n + 1$ is the number of crossings and

$$Q_1 = P_{\mathrm{LZ}}\big[P_{\mathrm{LZ}}\sin^2(\zeta_{12} + \zeta_{45} - \zeta_{24}) + (1 - P_{\mathrm{LZ}})(1 - \cos(\zeta_{15} + 2\phi_S)\cos(\zeta_{12} + \zeta_{45} - \zeta_{24}))\big], \tag{23}$$

$$Q_2 = 2P_{\mathrm{LZ}}(1 - P_{\mathrm{LZ}})\sin(\varphi_S + \zeta_{12} + \zeta_{45})\sin(\varphi_S + \zeta_{24}). \tag{24}$$

For both results, (19) and (22), it can be easily checked that the well-known results for an Hermitian Hamiltonian are recovered when $\delta \to 0$.

When the imaginary part of the potential is turned on ($\delta \neq 0$), our results clearly reflect the non-unitarity of the evolution by admitting $P_+ > 1$. Thus, P_+ should not be interpreted as a probability, but instead as the energy of the excited mode in units of the total initial energy of the light beam. Moreover, the direction in which the system first passes through the crossing is important, since it determines the sign of δ. These features are a direct consequence of the asymmetry of the two-level Hamiltonian (11), which in turn is a manifestation of the underlying non-Hermiticity of the system. The imaginary part of the $\mathcal{PT}$-symmetric potential $V_2 = \delta/2$ can be used to tune the desired outcome for the power in the excited state after several crossings as shown in figure 4. It is important to note that interferometry is also crucial for the control of the transitions. This is reflected in the maxima and minima observed in figure 4 where constructive and destructive interferences take place depending on the number of crossings and on the choice of δ.

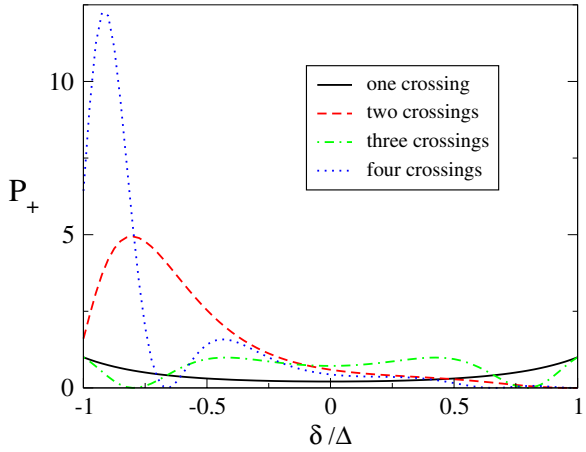

Figure 4. As the imaginary part of the $\mathcal{PT}$-symmetric potential is varied from $\delta = -\Delta$ to $\delta = +\Delta$, the resulting energies for the excited state are greatly modified. The chosen parameters are $\epsilon_0 = 0$, $\tilde{A} = 2$, $\tilde{\omega} = 0.02$ and $\Delta = 2V_1 = 0.2$.

It is interesting to further analyze the critical points where the gap of the system vanishes ($\delta^2 \to \Delta^2$). One possibility is to take the limit $\delta \to \Delta$ in (19) and easily obtain

$$P_+^{\text{even}}(n) = 0, \tag{25}$$

$$P_+^{\text{odd}}(n) = 1. \tag{26}$$

To understand this result, let us first remember that the system is initially prepared in its ground state for $\epsilon < 0$, which in the limit $\delta^2 \to \Delta^2$ is

$$v_{ini} = \begin{pmatrix} 1 \\ 0 \end{pmatrix}, \tag{27}$$

with eigenvalue ϵ. Since for any value of ϵ this state is an eigenstate, its evolution will consist in only a phase factor and the system remains in the same state. Thus, it is easy to see that for an odd number of crossings $\epsilon > 0$ and the state corresponds to the excited state; otherwise for an even number of crossings $\epsilon < 0$ and the system is found to be in the ground state.

Another way to reach criticality is by making $\delta \to -\Delta$:

$$P_+^{\text{even}}(n) = \frac{8\pi\Delta^2}{v}\sin^2(\Phi_{St})\frac{\sin^2(n(\zeta_{12}+\zeta_{45}-\zeta_{24}))}{\sin^2(\zeta_{12}+\zeta_{45}-\zeta_{24})} \tag{28}$$

$$P_+^{\text{odd}}(n) = 1. \tag{29}$$

In this regime, the upper off-diagonal element of the Hamiltonian becomes $H_{1,2} = 0$, so that the dynamics of the first component of the vector becomes independent of the second one. Actually, only the phase of this first term varies in time, which explains why the energy of the excited state remains constant for $\epsilon > 0$, i.e. for an odd number of crossings. On the other hand, the term $H_{2,1} = \Delta$ enables a gain process that is evident from the result for an even number of crossings. Furthermore, the expression for P_+^{even} reflects that if the velocity v diminishes there is more time for the gain process to take place, increasing the accumulated energy.

4. LZS interferometry in $\mathcal{PT}$-symmetric optical lattice

Advances in the realization of optical waveguide arrays with $\mathcal{PT}$-symmetric properties make the observation of interband transitions in $\mathcal{PT}$-symmetric periodic lattices a target within reach in the near future. As explained above, we are interested in interband transitions that are generated by the presence of a sinusoidal gradient in the refractive index.

In order to compare with the analytical results derived in the previous section, we will consider conditions such that the system dynamics occurs near one of the avoided energy crossings of the band structure of the complex lattice (see figure 2). The system is initially prepared in its ground state and then driven several times through the avoided level crossing. Beam splitting occurs at these scattering points due to non-adiabatic transitions and the intensity of the beam is modified in the process. We focus our analysis on the parameter window $0 < V_2 < V_2^{\text{crit}}$, where there are no singular or exceptional points, i.e. where two eigenfunctions coalesce into one [23]. As noted in section 2, the action of the fictitious periodic force in equation (2) can be effectively replaced in equation (7) by a Bloch-momentum $\tilde{q}$ that depends on z as

$$\tilde{q}(z) = \tilde{q}_0 + \tilde{A}\sin(\tilde{\omega}z), \tag{30}$$

with $\tilde{\omega} = \omega\lambda/\mathcal{E}_k$ and $\tilde{A} = 2A\tilde{\omega}\lambda k$. For simplicity, we will limit our analysis to the case where the driving is symmetric around the avoided crossing located at $\tilde{q} = 1$. As the initial state, we choose an input excitation that populates the lowest band with Bloch-momentum $\tilde{q}(z_i) = 1 - \tilde{A}$, at an initial position along the waveguides which we pick as $z_i = -\pi/4\tilde{\omega}$.

To obtain the occupation amplitude of the first excited band in our numerical calculations, the evolved state ψ_{q_f} needs to be projected onto the eigenstate of the corresponding band. Since this projection must conform with the orthonormality condition defined in (5), ψ_{q_f} is projected onto $\phi^{\dagger}_{q2}$, which is an eigenstate of $\mathcal{H}^{\dagger}$. In this regard, the projection coefficients can be calculated as

$$c_{q_f 2} = \int_{-\infty}^{\infty} \phi^{\dagger\,*}_{q_f 2}(x)\psi_{q_f}(x)\mathrm{d}x. \tag{31}$$

Recalling now that the evolved state with final Bloch-momentum q_f can be expanded as in equation (6) and $\phi^{\dagger}_{q2} = \sum_l b^{l\dagger}_{q2}\mathrm{e}^{\mathrm{i}(2kl+q)x}$ a straightforward calculation for the occupation probability of the excited mode yields

$$P = |c_{q_f 2}|^2 = \left|\sum_l b^{l\dagger *}_{q_f 2} a^l_{q_f}\right|^2. \tag{32}$$

We first consider a regime away from criticality, i.e. with a finite gap, and observe the evolution of the system both for the Hermitian ($V_2 = 0$) and non-Hermitian ($V_2 \neq 0$) cases. The power or occupation 'probability' of the excited mode is measured after each crossing at the points where the driving reaches its maxima. In figure 5, the results for the numerical simulations are compared with the corresponding analytical results coming from the two-level analytical approximation. Excellent agreement is observed between both results when $V_2 \neq 0$. Evidently, when the imaginary part of the potential is absent, the evolution is unitary and the occupation of the excited state remains below unity. Furthermore, as expected from equation (22), for an odd number of crossings the results for $V_2 = V_1/2$ and $V_2 = -V_1/2$ coincide. Comparison of figures 5(a) and (b) reveals that the results for an even number of crossings depend strongly on the sign of V_2, as predicted by the prefactor $(\Delta - \delta)/(\Delta + \delta)$ in equation (19). For $V_2 = 0$, the gap is larger making the analytical approximation less precise as seen in figure 5(c).

Now, let us consider getting very close to the critical limit $V_2^2 \to V_1^2$. In this regime, the gap between the lowest bands becomes very small at the Bragg-scattering points $q = k(1-2l)$.

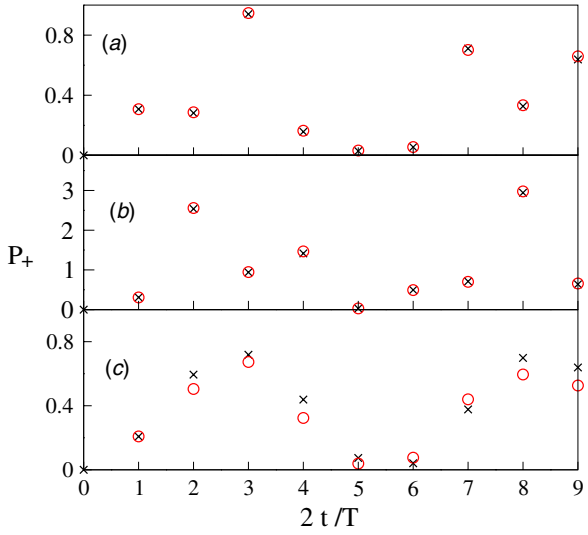

Figure 5. Energies of the excited state (or occupation 'probability') after each crossing away from criticality. Numerical results for the full system (circles) are compared to the analytical results obtained from the two-level approximation (crosses). The values chosen for the parameters are $\epsilon_0 = 0$, $\tilde{A} = 2$, $\tilde{\omega} = 0.02$ and $\Delta = 2V_1 = 0.2$. (*a*) $\delta = 2V_2 = 0.1$. (*b*) $\delta = 2V_2 = -0.1$. (*c*) $\delta = 2V_2 = 0$.

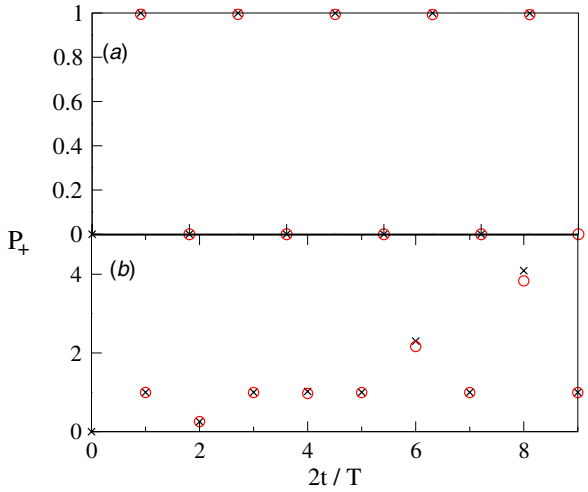

Figure 6. Energies of the excited state (or occupation 'probability') after each crossing near criticality. Numerical results for the full system (circles) are compared to the analytical results obtained from the two-level approximation (crosses). The values chosen for the parameters are $\epsilon_0 = 0$, $\tilde{A} = 3$, $\tilde{\omega} = 0.9$ and $\Delta = 2V_1 = 0.2$. (*a*) $\delta = 2V_2 = 1.999$. (*b*) $\delta = 2V_2 = -1.999$.

Figure 6 shows the numerical results for the occupation of the excited state after each crossing. Again, there is excellent agreement with the corresponding analytical results obtained using the two-level approximation derived in the previous section.

5. Concluding remarks

We have theoretically investigated the implementation of Landau–Zener–Stückelberg interferometry in $\mathcal{PT}$-symmetric complex lattices that could be realized in optical waveguide arrays. We studied first the effective two-mode system using the adiabatic-impulse approximation deriving analytical expressions for the power in the excited state. The expressions obtained were later compared with the numerical results for the complete multi-mode system driven periodically through an avoided crossing. Overall, we found that the two-mode framework provides accurate predictions and gives a complete understanding of the main features of the dynamics in the complex crystal under periodic driving.

We observed that the power transferred to the excited state is very susceptible to the speed of the system as it moves across the avoided level crossings, where the passage time determines the amount of energy gained/lost by the light beam. Also, the occupation of the excited state after several passages through one of the Bragg scattering points was shown to be particularly sensitive to the magnitude and sign of the imaginary part of the $\mathcal{PT}$-symmetric potential (V_2). Furthermore, the results exhibit strong dependence on the dynamical phases accumulated during the driving process due to the underlying LZS interference mechanism.

In summary, it is found that the LZS interference mechanism can be used as a powerful tool to control the intensity of the light beam in a complex waveguide array.

Acknowledgments

SAR and FAO acknowledge financial support from the FONDECYT project no. 11110537. LMM and SAR are also supported by the FONDECYT project no. 1110671.

References

[1] Shevchenko S N, Ashhab S and Nori F 2010 *Phys. Rep.* **492** 1
[2] Mark M, Kraemer T, Waldburger P, Herbig J, Chin C, Nägerl H-C and Grimm R 2007 *Phys. Rev. Lett.* **99** 113201
[3] Kling S, Salger T, Grossert C and Weitz M 2010 *Phys. Rev. Lett.* **105** 215301
Zenesini A, Ciampini D, Morsch O and Arimondo E 2010 *Phys. Rev.* A **82** 065601
[4] Huang P, Zhou J, Fang F, Kong X, Xu X, Ju C and Du J 2011 *Phys. Rev.* X **1** 011003
[5] Bender C 2007 *Rep. Prog. Phys.* **70** 947
[6] Moiseyev N 2011 *Non-Hermitian Quantum Mechanics* (Cambridge: Cambridge University Press)
[7] Sokolov A V, Andrianov A A and Cannata F 2006 *J. Phys. A: Math. Gen.* **39** 10207
[8] Bender C M and Boettcher S 1998 *Phys. Rev. Lett.* **80** 5243
[9] Bender C M, Brody D and Jones H 2002 *Phys. Rev. Lett.* **89** 270401
[10] Bender C M, Brody D and Jones H 2004 *Phys. Rev. Lett.* **93** 251601
[11] Dorey P, Dunning C and Tateo R 2001 *J. Phys.* A **34** 5679
[12] Dorey P, Dunning C and Tateo R 2007 *J. Phys. A: Math. Theor.* **40** R205
[13] Longhi S 2009 *Laser Photon. Rev.* **3** 243
[14] Della Valle G, Ornigotti M, Cianci E, Foglietti V, Laporta P and Longhi S 2007 *Phys. Rev. Lett.* **98** 263601
[15] Lenz G, Talanina I and de Sterke M C 1999 *Phys. Rev. Lett.* **83** 963
[16] Chiodo N, Della Valle G, Osellame R, Longhi S, Cerullo G, Ramponi R, Laporta P and Morgner U 2006 *Opt. Lett.* **31** 1651
[17] Rüter C E, Makris K G, El-Ganainy R, Christodoulides D N, Segev M and Kip D 2010 *Nature Phys.* **6** 192
[18] Longhi S 2009 *Phys. Rev. Lett.* **103** 123601
[19] Longhi S 2009 *Phys. Rev.* B **80** 235102
[20] Makris K G, El-Ganainy R, Christodoulides D N and Musslimani Z H 2008 *Phys. Rev. Lett.* **100** 103904
[21] Morales-Molina L and Reyes S A 2011 *J. Phys. B: At. Mol. Opt. Phys.* **44** 205403
[22] Shevchenko S N, Ashhab S and Nori F 2010 *Phys. Rep.* **492** 1
[23] Heiss W D 2004 *J. Phys. A: Math. Gen.* **37** 2455
Graeffe E M, Günter U, Korsh H J and Niederle A E 2008 *J. Phys. A: Math. Theor.* **41** 255206